Flash dry deposition of nanoscale material thin films

L. Hu,[a] G. Gruner,*[a] J. Jenkins[b] and C.-J. Kim[b]

Received 16th March 2009, Accepted 19th May 2009
First published as an Advance Article on the web 30th June 2009
DOI: 10.1039/b905318m

In this work, we report a simple and scalable solution-based method to deposit nanoscale material thin films. We have demonstrated uniform thin films fabricated by a flash dry deposition method, including carbon nanotubes and polyaniline nanofibers. The films are electrically uniform across an entire area of 8 inches by 8 inches in size. This method can be applied to other nanoscale materials and substrates or nanomaterial multilayer structures if the correct solution–substrate interface interaction is achieved. In the end, we use this method to deposit CNT thin films on an unusual substrate—the inner side of thin glass tubing. Such transparent and conductive coating in glass tubing is not possible with traditional indium tin oxide sputtering and allows for a novel design of electrowetting devices.

Introduction

Thin films made of randomly distributed nanoscale materials can be regarded as a new type of material. Collective behavior of nanostructures can provide unique physical properties and enhance device performance. Such thin films can be used to replace traditional materials with additional advantages. For example, transparent and conductive carbon nanotube (CNT) thin films can be used to replace indium tin oxide (ITO) in optoelectronics which brings in additional mechanical flexibility.[1,2] From a production point of view, replacing traditional materials with nanoscale material thin films can have another advantage in that thin film coatings, especially of inorganic materials, typically require high vacuum and high temperatures, which limit the choice of substrate to those with high cost. A solution-based, low temperature fabrication method can be used to deposit nanoscale thin films, which obviates the need for vacuum and high temperatures. In addition to the emergent functionalities of nanoscale materials, this sharp contrast with vacuum-based methods makes the choice of using solution-based nanoscale thin films attractive.

There are various well-developed solution-based coating methods, such as self-assembly of monolayers (SAM), Langmuir–Blodgett (LB) assembly, electroplating, spraying, spin coating, dip coating, slit coating, and ink-jet printing, among many others.[3–8] All of these solution-based coating methods can be applied toward the fabrication of nanoscale material thin films. Some coating methods, such as spin coating, are widely used in microfabrication and some can be applied in a roll-to-roll fashion to achieve a large scale fabrication of nanoscale material thin films. Solution–substrate interface interaction is critical for achieving a uniform coating of nanoscale materials. For example, saline functionalization is used for CNT thin film deposition to enhance the interaction between the CNT and substrate to avoid peeling of the film during the washing step for removing surfactants.[9] Another critical factor for solution-based coating is a controlled drying process. For example, the dip coating method has been used to coat CNT thin films, however, micro domains or crystal-shaped structures were formed.[10] One major reason for the appearance of the cluster feature is most likely due to the uneven and badly controlled drying process. In this paper, we present a controlled drying method for fabricating nanoscale material thin films. Uniform CNT or polyaniline (PANI) nanofiber thin films on plastic PET and glass substrates have been demonstrated.

Experimental and results

Fig. 1 (a) illustrates the setup and basic principle of the solution-based flash dry deposition method. A nanomaterial solution is applied to the substrate first, and then a heating bar passes over the liquid to force the drying in a controlled way. The thickness of the solution is in the range 10 to 100 μm which can be applied by various methods, such as Meyer rod coating, dip coating or spin coating. The wet thickness of the nanomaterial solution is controlled by the Meyer rod size, dip coating speed or spin coating speed. The final thickness of the nanoscale material thin film is determined by the concentration and the wet liquid thickness. The heating bar moves from one edge toward the other with a speed that allows full drying of the liquid in the area it passes. Such control of drying forms a clear interface between the dried film and the liquid, which continues to move along with the heating bar. In this fashion, the heat line formed in the wet liquid force a uniform drying on the surface. There is no agglomeration formed during the drying process, resulting in a uniform nanomaterial coating. The only pre-condition of such a method is the uniformity of the liquid coating, which can be easily met by the previous mentioned methods. The stringent requirement of the liquid–substrate interaction associated with dip coating is not attendant in this flash dry method.

We applied this concept for CNT thin film deposition on various substrates. The CNT dispersion preparation details are documented in our previous publication.[11] Briefly, 1 mg mL^{-1} laser ablation single walled nanotubes were dispersed in water with 1% by weight Triton X as a surfactant, followed by probe sonication. Centrifugation at 3000 rpm was used to remove large

[a]*Department of Physics, University of California, Los Angeles, 90095, USA. E-mail: gruner@physics.ucla.edu*
[b]*Department of Mechanical and Aerospace Engineering, University of California, Los Angeles, 90095, USA*

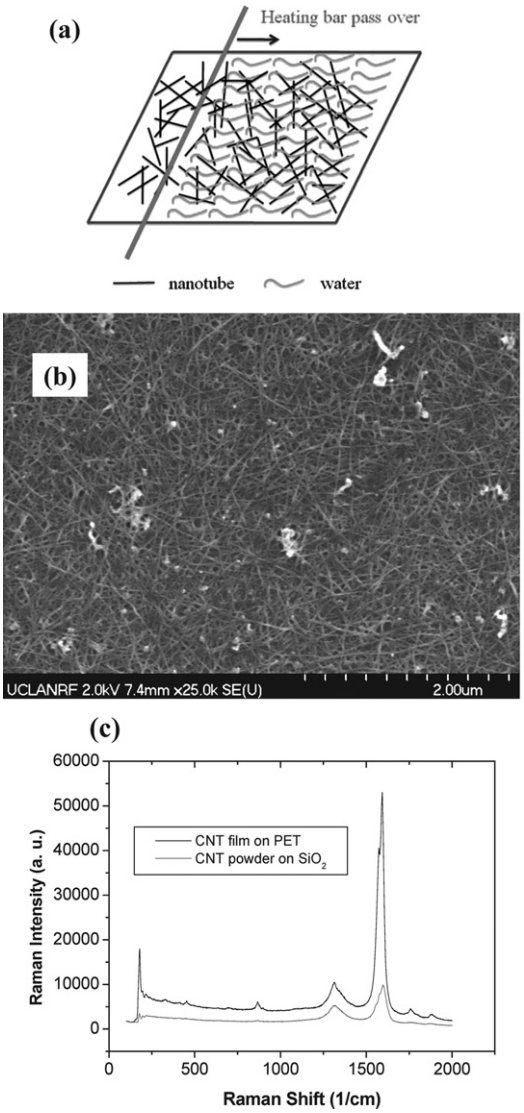

Fig. 1 (a) Flash dry deposition scheme. As the heating bar passes the thin CNT liquid, it forces the evaporation of water and leaves the dry CNT and surfactant on the substrate. (b) SEM image of CNT thin film on PET substrate deposited with the flash dry deposition method. (c) Raman spectra of CNT thin film coated on PET and starting CNT powder on SiO_2.

bundles in solution. Then the solution is applied to a polyethyleneterephthalate (PET) or glass substrate using the Meyer rod method. The resulted liquid coating is 10 μm thick. We also tried the dip coating method by immersing the substrate in the dispersion followed by gradually pulling the substrate from the liquid. A tremendous amount of liquid, approximately 2 litres, is required for dip coating an 8 inch by 8 inch sample, while only 1 mL of liquid is required for the Meyer rod method. After the coating of liquid on the surface, an infrared (IR) lamp with 2200 W of power is gradually moved across the web of CNTs. The constant distance between the web and the substrate is held at 3 inches and the speed of the IR lamp is 5 inches per min. The substrate sizes are 8 inches by 8 inches. After the IR lamp moves across the substrate, uniform films are present on the substrate. To achieve high conductivity, removal of the surfactant with water is needed. The substrate surface is pretreated with silane to achieve enough adhesion for the film to survive the washing process. The films are soaked in water for two min and then blown dry with nitrogen. The sheet resistance is measured with a standard four point probe machine. Sheet resistance of 400 Ohm sq^{-1} and transmittance of 85% at 550 nm are achieved. The film thickness based on an AFM study is approximately 20 nm for CNT films. The performance of transparent and conductive CNT films in this study is close to the performance of ITO on a plastic substrate which is enough for voltage driven devices. The calculated conductivity based on our previous model for single walled CNT is 1110 S cm^{-1}.[1] The sheet resistance is uniform across the web, with a standard deviation of less than 5%. Fig. 1 (b) shows a SEM image of the film on a PET substrate deposited with flash drying. The film shows a homogenous structure with a uniform bundle distribution. There are no agglomerations formed, as probed by SEM and microscope imaging. We also evaluated the Raman spectrum of a CNT film on PET and compared it with the starting CNT powder on a SiO_2 substrate using a 785 nm laser with a Renishaw Raman spectrometer, Fig. 1 (c). The two most prominent features are a low-frequency radial breathing mode (RBM) located at 178 cm^{-1} and a high-frequency G-band at 1593 cm^{-1} that are at identical positions, indicating no damage of CNT films using the IR to dry the film.

For comparison purposes, the other two types of drying are explored in this study. First, after the coating of a CNT liquid on a PET or glass substrate, the sample is put onto a hot plate to dry. We found that large clusters with sizes of millimetres to centimetres are formed during the drying. The dried film is visually not uniform with areas of black and white randomly distributed on the substrate. This may be due to the non-uniformity of the surface properties, substrate heating, or due to surface tension. One typical pattern formed is that of Bénard cells with randomly distributed sizes on the order of a few millimetres. Additionally, we tried using the IR lamp on a liquid coating without moving it from one edge to the other. We found the resulting film to be non-uniform also. We observed that the moving IR bar causes a dynamic drying line in the CNT coating between dried and wet areas. The interface line moves at the same speed as the IR lamp and forces drying without any agglomeration. Others have also used the dip coating method to coat CNT thin films on substrates, but without the use of the moving IR lamp. In their study, the CNTs form large domains and cluster-like structures. The slow drying that occurred with these samples allowed the formation of macrostructures in the film, and no homogenous films were achieved.[10]

Flash dry deposition allows for a quick and controlled deposition method for CNT thin films. More importantly, this method is scalable for large size film fabrication. For deposition of CNTs on a large scale, spray coating has been developed in industry and academia, likely due to dip coating's lack of control of heating appropriate to the specific CNT formulation used.[9–12] The film microstructures of sprayed films and flash-dried films are compared. Fig. 2 (a) and (b) show the AFM of CNT films on glass substrates deposited with flash drying and spray methods, respectively. It is clear that the flash drying method leads to a much more homogenous film than the spraying method does. There are micrometre sized holes in the spray-coated CNT films,

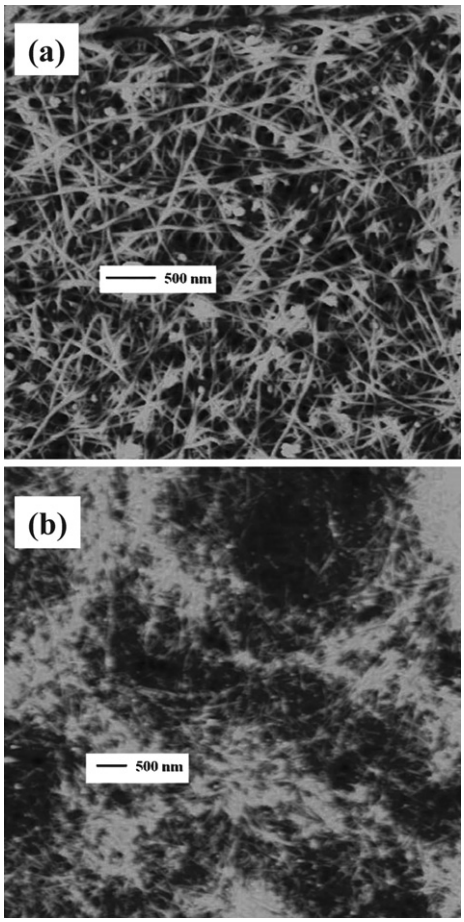

Fig. 2 (a) AFM image of a CNT thin film on a glass substrate deposited using the flash dry deposition method. (b) AFM image of a CNT thin film on a glass substrate deposited using the spray coating method.

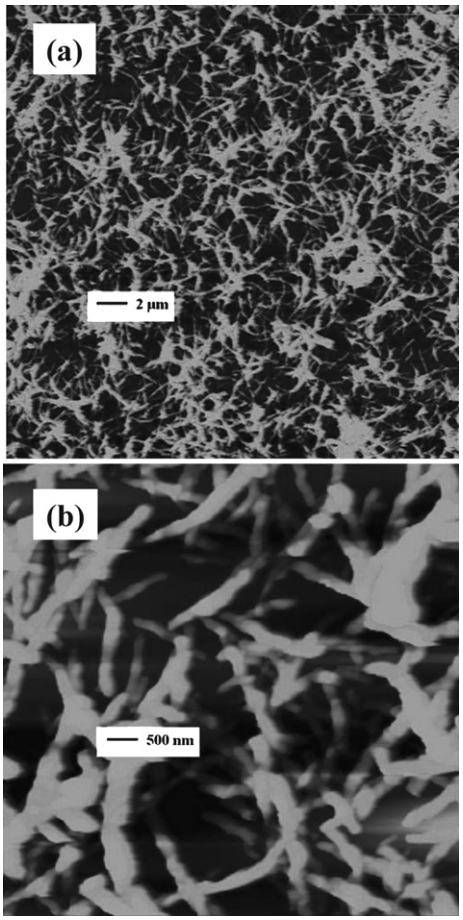

Fig. 3 (a) AFM image of a PANI nanofiber thin film deposited on a PET substrate using the flash dry deposition method. (b) A higher magnification image of a PANI nanofiber thin film deposited on a PET substrate to show the film structure.

with an average diameter of 1–2 μm. During the spray coating method, the substrate is heated to 120 °C to evaporate the liquid quickly. The details of the spraying method are detailed in our previous publication.[11] The formation of the micro size holes comes from the nature of the spraying method. The mist of liquid emitted from the spraying nozzle is composed of droplets of approximately 20 μm in diameter. These mist droplets are spherically-shaped while in air and circular after drying on the substrate. When these circular-shaped areas interconnect with each other, a uniform film is formed on the substrate. However, the nature of overlapping of disk-shaped areas leads to holes in the film. To avoid this problem, a solution with low concentration can be used, but more spraying steps are required to form a relatively more homogenous film, compared with concentrated CNT solutions.

We also applied the flash deposition method to fabricate other nanoscale material thin films, one example being conductive PANI nanofibers. A PANI nanofiber solution was prepared by following ref. 13. The same deposition method is applied here but the PET and glass substrates are without pretreatment. The concentration of PANI fibers is 0.5 mg mL^{-1} and the IR bar speed is 4 ft per min. Fig. 3 (a) shows the AFM image of PANI fibers fabricated on a glass substrate. The film is homogenous across the imaging area. Mapping the sheet resistance of the nanofiber film, we found that we achieved good uniformity of the film across the 8 inch by 8 inch sample, with a standard deviation of sheet resistance less than 6%. The PANI nanofiber film thickness was probed by AFM and was 35 nm. Fig. 3 (b) shows the microstructure of the film where the PANI nanofibers interpenetrate each other. Without the use of the moving heat bar, but with the use of the hot plate, the PANI forms a few millimetre-long line defects.

Deposition of nanomaterial thin film on unusual substrates can allow for novel design of devices. Devices utilizing electrowetting—most commonly in the form of electrowetting-on-dielectric (EWOD)—intended for lab-on-a-chip applications typically translate small droplets of liquid squeezed between two planar, parallel plates for ease of integration[14] as shown in Fig. 4 (a). Since the droplets are guided by virtual sidewalls defined only by electric signals, rather than being confined to physical channels, their movement cannot be used to build any pressure. Some devices, however, may seek to harness the pressure generated by the moving droplets. The droplet under actuation may do work upon another, solid component of the device, or translate the pressure hydraulically through an immiscible fluid. This scheme could be utilized in the development of lab-on-a-chip systems, medical micro dosing drug

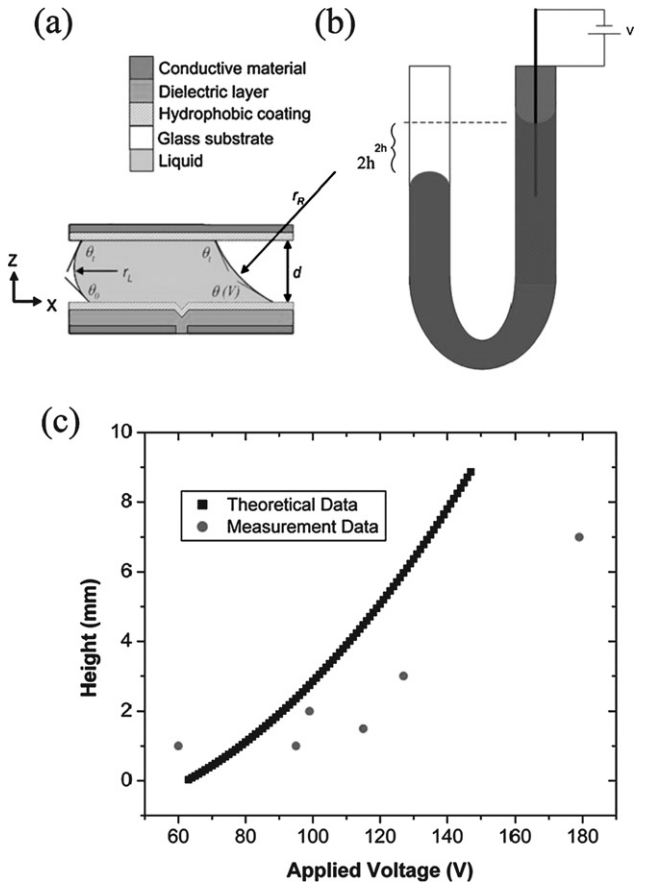

Fig. 4 (a) Typical device configuration of EWOD, which has parallel plates. (b) Tubular EWOD device with a transparent CNT thin film coated on the inner side of glass tube using the flash dry deposition method; the dielectric layer is approximately 2 μm thick parylene-C and the hydrophobic coating is approximately 200 nm thick Teflon. CNT thin film is the conductive material. (c) Liquid height-of-rise performance with applied voltage. All voltage values are DC.

delivery devices, or any other system that depends on a micropump.[15] Such applications would not be well-served by the open, expansive parallel plate geometry of common EWOD devices. The droplet and any hydraulic fluid must be tightly contained in order to direct the application of force. Microchannels fabricated on the planar substrate are one way of providing containment, but typically bear a square-shaped cross-section due to the planar fabrication processes used. A droplet moving inside the square channel may not be effective in building pressure due to leakage in the inner corners of the channel that are unfilled by the droplet. A more efficient translation of pressure requires a channel with circular cross-section, which the droplet completely fills at all times. Furthermore, since a droplet is actuated at its menisci on the electrodes, wrapping the electrode all around the circumference of the droplet should result in more actuation force and more efficient pressure generation for the voltage applied. Unfortunately, however, sputtering does not provide the degree of conformity needed to coat the inner surfaces of a capillary tube with a metal.

Here we demonstrate the deposition of a CNT thin film on the inner surfaces of glass tubing and introduce an EWOD device made from a round tube. Fig. 4 (b) shows the device schematic. It is the first time that an electrowetting device has been fabricated in a tubular structure. The inner diameter of the glass tubing is 2 millimetres and the length is approximately 3 centimetres. To deposit the CNT thin film, the tube is filled with the CNT solution while one end is blocked. The blocked side is then released. A thin layer of liquid is left uniformly on the glass tubing, both inside and out. The outside is wiped off and the tubing is laid down horizontally on a plate. The IR heat bar moves across the glass tubing with controlled speed so that the liquid dries as the IR bar moves across. After this, the tubing was soaked in water to remove the surfactant. The resistance of the tubing is evaluated by a multimeter, with one probe on one side of the tubing and the other probe on the opposite side. The resistance reading was nominally 2 kOhm. The tubes were additionally coated with a conformal layer of parylene-C, approximately 2 μm thick, at the UCLA nanofabrication laboratory. While other dielectrics such as silicon oxide or silicon nitride may be used, they are coated by CVD systems that do not provide enough conformity to accommodate the inner surface of a tube. Pellets of parylene-C are vaporized in a furnace at 690 °C and deposited on the samples in a bell chamber at 135 °C and 25 mTorr pressure. To make the interior surface hydrophobic, the tubes were then dip-coated in an AF 1600 Teflon solution for an approximate film thickness of 200 nm, as measured by a profilometer on similarly dip-coated planar samples, and annealed at 200 °C.

To test the feasibility of electrowetting in a circular channel, we constructed a u-tube manometer using a CNT-coated glass tube and another glass tube coated only with a Teflon solution for hydrophobicity, connected by Tygon tubing and filled with deionized water. The CNT film acted as the actuation electrode, with a concentric metal needle inserted to act as the grounding electrode. During experimentation, the device is held vertically. The tube without the CNT coating is not actuated. Upon application of voltage, the meniscus in the actuated, CNT-coated side of the device climbs the tube (while the meniscus in the other tube conversely descends) until it saturates at a constant height as shown in Fig. 4 (b). The stable height change of the leading meniscus was measured at discrete DC voltages. Fig. 4 (c) shows the performance of the liquid height *versus* applied voltage. Theoretical height change with voltage is plotted along with the data. The equation is obtained by assuming that, at equilibrium where the height change is measured, the pressure generated by EWOD actuation is equal and opposite to the sum of the negating hysteresis pressure and the hydrostatic pressure difference between the displaced menisci.

$$h = \frac{\left[\frac{cV^2}{r} - P_{\text{hysteresis}}\right]}{2\rho g} \quad (1)$$

The actuation pressure term is derived from an application of the Lippmann–Young and Laplace equations to the tubular geometry and material properties of the devices, with V the applied voltage, r the inner radius of the tube (1 mm) and c equal to the specific capacitance of the dielectric layer

$$c = \frac{\varepsilon_0 K}{t} \quad (2)$$

where ε_0 is the permittivity of free space (8.854×10^{-12} s^4 A^2 m^{-3} kg^{-1}), κ is the dielectric constant of parylene-C (2.7) or Teflon (1.9) and t is the thickness of the dielectric layer (1.97 μm parylene-C and 200 nm Teflon). The application of voltage changes the effective contact angle between the water and the tube surface, and the resulting difference in curvature between the menisci in either end of the device establishes a pressure gradient within the liquid, causing it to move within the tubes.[14,16] It has been shown that contact angle hysteresis can be represented as a constant friction term[17–19]

$$P_{\text{hysteresis}} = \frac{2\gamma_{\text{lg}}\left[\cos(\theta_{\text{r}}) - \cos(\theta_{\text{a}})\right]}{\pi r} \quad (3)$$

where γ_{lg} is the surface energy of the water–air interface (73 J m^{-2}), r is the radius of the tube (1 mm) and θ_{a} and θ_{r} are the advancing and receding contact angles, measured as 125° and 115°, respectively.

The data are seen to follow the general trend of the theoretical prediction, but underperform the prediction at most points, which is likely attributable to non-uniformity and uncertainty of the dielectric thickness on the inner surface as well as surface variations such as holes and roughness due to imperfections in materials coating processes. Such non-ideal features demand higher EWOD driving voltages and increased droplet hysteresis, working against the electrowetting actuation.[17,19,20]

Conclusion

We reported a quick and controlled method for fabricating nanoscale material thin films on various substrates. The concept was illustrated with examples of deposited CNT and PANI nanofiber thin films on PET and glass substrates. This method leads to uniform films over macroscale areas by visual observation and homogenous structures in the microscale by SEM or AFM imaging. The controlled drying in this method prevents agglomeration due to the uneven distribution of heat, surface morphology or surface energy. The drying method can be extended to a linear heat bar or IR laser. The solution–substrate interface formation is critical for this method. This method can be applied to other nanoscale material thin film coatings, without the stringent requirement of the formation surface energy and surface interaction with the substrate. Also, the method can be used to form multilayer structures or interpenetrated networks for achieving various functionalities.

Acknowledgements

This work is supported by NSF Grant No. DMR-0404029.

References

1 L. Hu, D. S. Hecht and G. Gruner, *Nano Lett.*, 2004, **4**, 2513.
2 Z. Wu, Z. Chen, X. Du, J. M. Logan, J. Sippel, M. Nikolou, K. Kamaras, J. R. Reynolds, D. B. Tanner, F. Hebard and A. G. Rinzler, *Science*, 2004, **305**, 1273.
3 A. Ulman, Formation and structure of self-assembled monolayers, *Chem. Rev.*, 1996, **96**, 1533.
4 M. Tirrell and A. Katz, Self-assembly in material synthesis, *MRS Bull.*, 2005, **30**, 700.
5 A. Ulman, *An introduction to ultrathin organic films from Langmuir-Blodgett to self-assembly*, Academic Press, Inc., San Diego, 1991.
6 J. A. Brogan, *MRS Bull.*, 2000, **25**, 48.
7 M. Kaempgen, G. Duesberg and S. Roth, *Appl. Surf. Sci.*, 2005, **252**, 425.
8 M. Lima, M. Andrade, C. Bergmann and S. Roth, *J. Mater. Chem.*, 2008, **18**, 776.
9 J. Liu, M. Casavant, M. Cox, D. Walters, P. Boul, W. Lu, A. Rimberg, K. Smith, D. Colbert and R. Smalley, *Chem. Phys. Lett.*, 1999, **2**, 125.
10 Y. Yan, M. B. Chan-Park and Q. Zhang, *Small*, 2007, **3**, 24.
11 L. Hu, G. Gruner, J. Gong, C.-J. Kim and B. Hornbostel, *Appl. Phys. Lett.*, 2007, **90**, 093124.
12 T. M. Barnes, J. van de Lagemaat, D. Levi, G. Rumbles, T. J. Coutts, C. L. Weeks, D. A. Britz, I. Levitsky, J. Peltola and P. Glatkowski, *Phys. Rev. B*, 2007, **75**, 235410.
13 J. Huang and R. B. Kaner, *Angew. Chem., Int. Ed.*, 2004, **43**, 5817.
14 J. Lee, H. Moon, J. Fowler, T. Schoellhammer and C.-J. Kim, *Sens. Actuators, A: Phys.*, 2002, **95**, 2–3.
15 K. S. Yun, I. J. Cho, J. U. Bu, C.-J. Kim and E. Yoon, *J. Microelectromech. Syst.*, 2002, **11**, 5.
16 H. Moon, S. K. Cho, R. Garrell and C.-J. Kim, *J. Appl. Phys.*, 2002, **92**, 7.
17 C. G. L. Furmidge, *J. Colloid Sci.*, 1962, **17**, 309.
18 W. Shen, J. Kim, and C.-J. Kim, *Proc. ASME IMECE*, New York, NY, 2001.
19 E. B. Dussan and R. T. P. Chow, *J. Fluid Mech.*, 1985, **151**, 1.
20 S. K. Cho, H. Moon and C.-J. Kim, *J. Microelectromech. Syst.*, 2003, **12**, 70.